A Modular Aerogel Imaging Cerenkov Counter

J. M. Durham[a], H. W. van Hecke[a]

[a]*Los Alamos National Laboratory, Los Alamos, NM 87545, USA*

Abstract

A new silicon detector has been developed to provide xxx momentum of 5 GeV/c will allow identification of muons from relatively long-lived particles, such as D and B mesons, through their broader DCA distributions.

Keywords: RHIC, PHENIX, FVTX, silicon detector
PACS: 29.40.Wk, 25.75.Nq, 14.20.Dh

1. Introduction

A new silicon tracking detector has been developed and installed in the PHENIX detector at the Relativistic Heavy Ion Collider (RHIC). xxx

on the FVTX silicon sensors are discussed in Section 4, and Section 5 shows the initial performance of the detector during RHIC's 2012 and 2013 run periods.

2. Mechanical Design

A schematic diagram of a focusing Cerenkov detector is shown in Fig. 1 A Cerenkov radiator of thickness t is followed at a distance d by a focusing element, typically a mirror or a lens, and an imaging plane at distance f from the focusing element. A Cherenkov ring with radius r is formed in the image plane, where a photon detector registers the Cerenkov light. This detector may also register the passage of the charged particle at p. The image in the focal plane is independent of d, and we set this distance to zero. The ring radius r is determined by the Cerenkov angle and by the focal length f of the focusing element:

r = f*tan(theta)

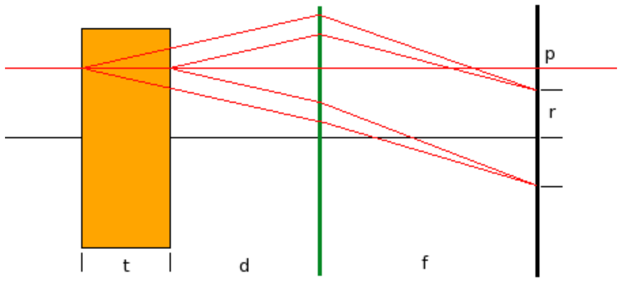

Figure 1: A diagram of an generic imaging Cerenkov counter: a radiator of thickness t, followed by an imaging element (green) of focal length f, and a photon detector (black).

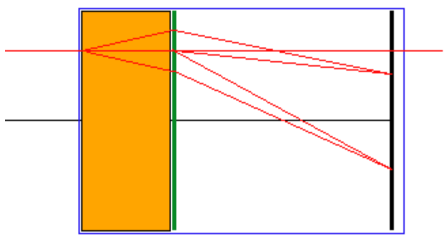

Figure 2: The imaging element is placed against the exit surface of the radiator, and all elements are enclosed in a box with mirror surfaces.

Fig. 2 shows the radiator, focusing elements, which is taken to be a lens, and the photon detector plane, all enclosed in a box. Under certain conditions, namely when incident particle paths make an angle with the horizontal greater than the Cerenkov angle, or when the incident particle is very close to the boundary, some of the photons will hit the box wall. If the inside surfaces of the box are made of flat mirror material, these photons will not be lost. The pattern formed in the image plane may be distorted as in Fig. 3, but these are shapes that can be recognized by the pattern recognition software.

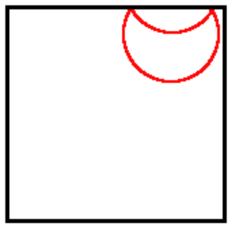

Figure 3: If an incident particle makes a large angle wrt the optical axis, the Cerenkov ring in the image plane may become folded.

Fig. 4 shows the how several units can be arranged into a projective geometry to form a relatively shallow, self-contained wall.

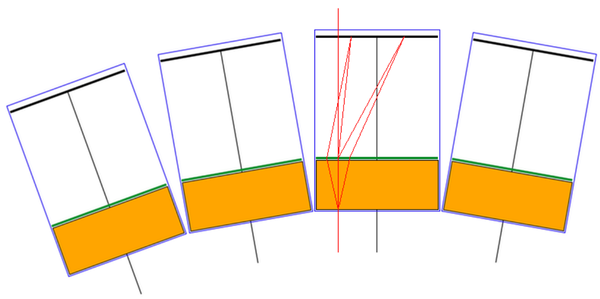

Figure 4: Individual units may be stacked to make a hermetic, projective detector wall.

*Corresponding author. E-mail address: hubert@lanl.gov

2.1. Radiator choice

If we want to distinguish Kaons from pions in the few-GeV range, the refractive index of the Cerenkov radiator needs to be in the 1.01-1.02 range as can be seen in Fig. 5, and the only material with such indices is silica

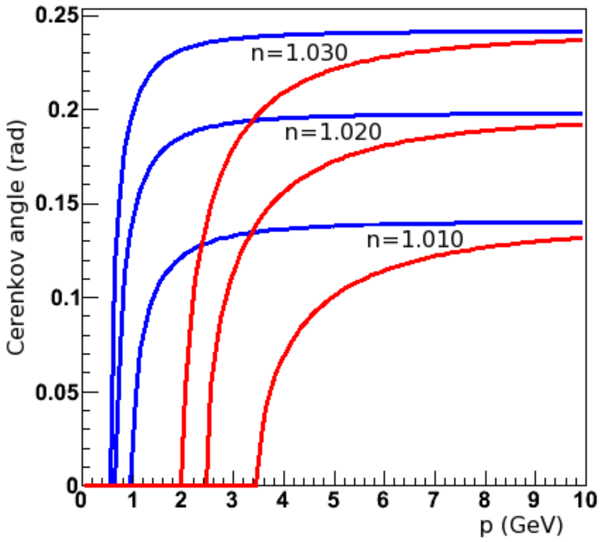

Figure 5: Threshold curves for Kaons (red) and pions (blue) for different refractive indices.

aerogel. Fig. 6 shows a Cerenkov ring produced using a 450 GeV proton beam. The outer ring is formed by Cerenkov radiation from n=1.010 aerogel, and the small ring in the center results from Cerenkov radiation from air in the detector. Photons in aerogel are subject to Rayleigh scattering, which scales as $\lambda^{-}4$, where λ is the wavelength. Fig. 7 shows a transmission spectrum of a 3 cm thick sample of aerogel (histogram). The transmission spectrum can be parametrized by

T = A*exp(Cxxx/lambda-4)

where A is the transmission at large wavelength, and C (for 'clarity') is a measure of the quality of the sample - the lower C, the more photons exit unscattered.

Photons in the Cerenkov ring are those that are not scattered before exiting the aerogel. This favors photons at long wavelengths, and photons produced close to the exit surface of the radiator. Fig. 8 shows in the left panel a typical spectrum of produced Cerenkov photons, falling with λ2. In the right panel are shown the spectra of scattered and unscattered

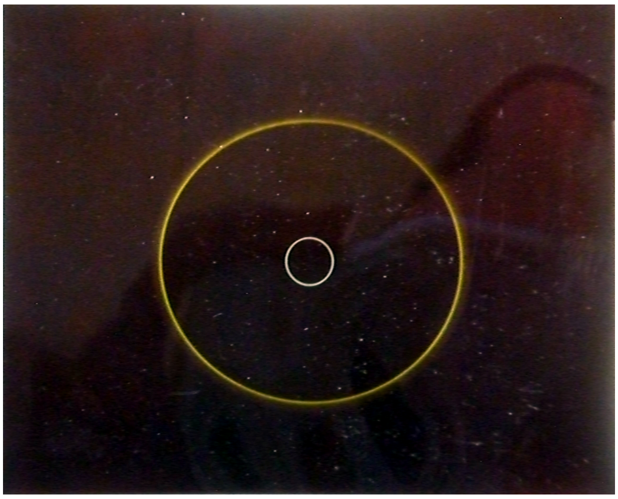

Figure 6: Threshold curves for Kaons (red) and pions (blue) for different refractive indices.

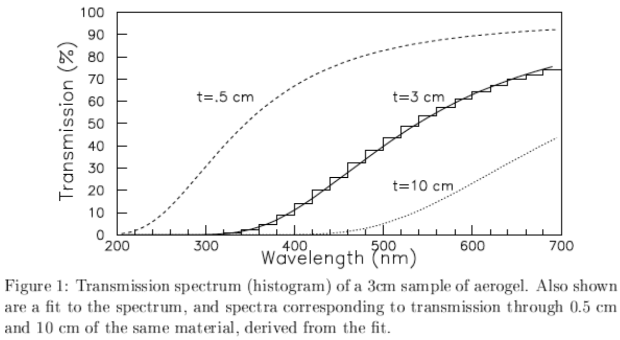

Figure 7: Transmission spactrum (histogram) of a sample of aerogel.

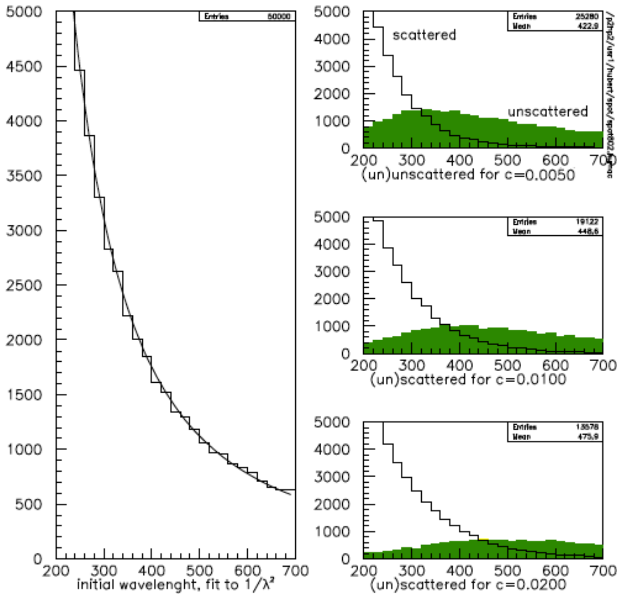

Figure 8: Left: spectrum of produced Cerenkov photons. Right: spectra of scattered (histogram) / unscattered (green) photons, for different values of the aerogel parameter C.

photons for aerogel of different values of the clarity C. The distributions of unscattered photons have a broad maximum at wavelengths in the 300-500 nm range, and their number increases with decreasing values of C.

2.2. The Focusing Element

In most focusing Cerenkov detectors currently in use, the element that focuses the Cerenkov photons into a ring is a concave mirror, or a set of such mirros. In such cases the detector plane may need to be placed to the sides of the radiator volume, which makes hermetic, modular construction impossible.

In this proposal, this element is an acrylic Fresnel lens. These typically are 1 mm thick or less. A transmission spectrum of such a lens is shown in Fig. 9. Such a lens would absorb most of the scattered photons, and pass most, though not all, of the unscattered photons.

2.3. The Photon Detector

(VTX) [1], and in front of the north and south muon

[1] A. Taketani, et al., Nucl. Instrum. Meth. A 623 (2010) 374–376.

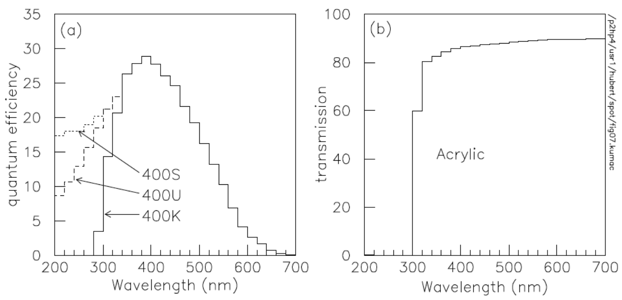

Figure 13: Quantum efficiency of the EMI9125 PMT (a), and transmission spectrum of the UV-acrylic of the fresnel lenses (b).

Figure 9: Left: Sensitivity spectra of selected Hamamatsu photocathodes. Right: transmission spectrum of a acrylic fresnel lens.